

WSRC-TR-97-0031

**HELIUM EMBRITTLEMENT MODEL
AND PROGRAM PLAN FOR WELDABILITY
OF ITER MATERIALS (U)**

By

**M. R. Louthan, Jr.
W. R. Kanne, Jr.
M. H. Tosten
D. T. Rankin
B. J. Cross**

FEBRUARY, 1997

A report written in support of the International
Thermonuclear Experimental Reactor (ITER)
under Task Agreement G15TT126-05-15FR,
Subtask 5, Phase 1.

DISTRIBUTION OF THIS DOCUMENT IS UNLIMITED

**Westinghouse Savannah River Company
Aiken, SC 29808**

PREPARED FOR THE U.S. DEPARTMENT OF ENERGY
UNDER CONTRACT DE-AC09-96SR18500

MASTER

DISCLAIMER

This report was prepared as an account of work sponsored by an agency of the United States Government. Neither the United States Government nor any agency thereof, nor any of their employees, makes any warranty, express or implied, or assumes any legal liability or responsibility for the accuracy, completeness, or usefulness of any information, apparatus, product, or process disclosed, or represents that its use would not infringe privately owned rights. Reference herein to any specific commercial product, process, or service by trade name, trademark, manufacturer, or otherwise does not necessarily constitute or imply its endorsement, recommendation, or favoring by the United States Government or any agency thereof. The views and opinions of authors expressed herein do not necessarily state or reflect those of the United States Government or any agency thereof.

This report has been reproduced directly from the best available copy.

Available to DOE and DOE contractors from the Office of Scientific and Technical Information, P. O. Box 62, Oak Ridge, TN 37831; prices available from (423) 576-8401.

Available to the public from the National Technical Information Service, U. S. Department of Commerce, 5285 Port Royal Rd., Springfield, VA 22161

DISCLAIMER

**Portions of this document may be illegible
in electronic image products. Images are
produced from the best available original
document.**

Acknowledgment

This report is an account of work assigned to the U.S. Home Team under Task Agreement No. G15TT126-05-15FR within the Agreement among the European Atomic Energy Community, the Government of Japan, the Government of the Russian Federation, and the Government of the United States of America on Cooperation in the Engineering Design Activities for the International Thermonuclear Experimental Reactor ("ITER EDA Agreement") under the auspices of the International Atomic Agency (IAEA). The report has not been reviewed by the ITER Publications Office.

ITER Disclaimer

This report is an account of work undertaken within the framework of the ITER EDA Agreement. Neither the ITER Director, the Parties to the ITER Agreement, the U.S. DOE, the U.S. Home Team Leader, the U.S. Home Team, the IAEA or any agency thereof, or any of their employees, makes any warranty, express or implied, or assumes any legal liability or responsibility for the accuracy, completeness, or usefulness of any information, apparatus, product, or process disclosed, or represents that its use would not infringe privately owned rights. Reference herein to any specific commercial product, process, or service by trade name, trademark, manufacturer, or otherwise, does not necessarily constitute or imply its endorsement, recommendation, or favoring by the parties to the ITER EDA Agreement, the IAEA or any agency thereof.

The views and opinions of authors expressed herein do not necessarily state or reflect those of the ITER Director, the Parties to the ITER Agreement, the U.S. DOE, the U.S. Home Team Leader, the U.S. Home Team, the IAEA or any agency thereof.

WSRC/DOE Disclaimer

This report was prepared as an account of work sponsored by an agency of the United States Government. Neither the United States Government nor any agency thereof, nor any of their employees, makes any warranty, express or implied, or assumes any legal liability or responsibility for the accuracy, completeness, or usefulness of any information, apparatus, product, or process disclosed, or represents that its use would not infringe privately owned rights. Reference herein to any specific commercial product, process, or service by trade name, trademark, manufacturer, or otherwise does not necessarily constitute or imply its endorsement, recommendation, or favoring by the United States Government or any agency thereof. The views and opinions of authors expressed herein do not necessarily state or reflect those of the United States Government or any agency thereof.

SMTD
STRATEGIC MATERIALS TECHNOLOGY DEPARTMENT

Keywords: Helium Embrittlement
Stainless Steel
Weld Cracks

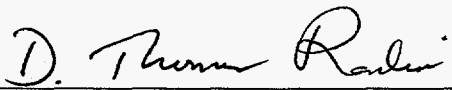
Retention: Permanent

**HELIUM EMBRITTLEMENT MODEL
AND PROGRAM PLAN FOR WELDABILITY
OF ITER MATERIALS (U)**

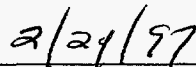
by

M. R. Louthan, Jr.
W. R. Kanne, Jr.
M. H. Tosten
D. T. Rankin
B. J. Cross

ISSUED: FEBRUARY 1997



Authorized Derivative Classifier



Date

SRTC SAVANNAH RIVER TECHNOLOGY CENTER, AIKEN, SC 29808
Westinghouse Savannah River Company
Prepared for the U. S. Department of Energy under Contract DE-AC09-96SR18500

DOCUMENT: WSRC-TR-97-0031

TITLE: HELIUM EMBRITTLEMENT MODEL AND PROGRAM
PLAN FOR WELDABILITY OF ITER MATERIALS

APPROVALS

M. R. Louthan, Jr., AUTHOR
MATERIALS TECHNOLOGY SECTION

DATE: _____

W. R. Kanne, Jr., AUTHOR
MATERIALS TECHNOLOGY SECTION

DATE: _____

M. H. Tosten, AUTHOR
MATERIALS TECHNOLOGY SECTION

DATE: _____

D. T. Rankin, AUTHOR
MATERIALS TECHNOLOGY SECTION

DATE: _____

B. J. Cross, AUTHOR
STRATEGIC PROGRAMS AND PLANNING

DATE: _____

S. L. West, TECHNICAL REVIEWER
MATERIALS TECHNOLOGY SECTION

DATE: _____

T. L. Capeletti, MANAGER
MATERIALS TECHNOLOGY SECTION

DATE: _____

**HELIUM EMBRITTLEMENT MODEL
AND PROGRAM PLAN FOR
WELDABILITY OF ITER MATERIALS**

by

M. R. Louthan, Jr.
W. R. Kanne, Jr.
M. H. Tosten
D. T. Rankin
B. J. Cross

Westinghouse Savannah River Co.
Aiken, SC 29808

January 1997

In fulfillment of ITER Task Agreement
G15TT126-05-15FR, Subtask 5, Phase 1

ABSTRACT

This report presents a refined model of how helium embrittles irradiated stainless steel during welding. The model was developed based on experimental observations drawn from experience at the Savannah River Site and from an extensive literature search. The model shows how helium content, stress, and temperature interact to produce embrittlement. The model takes into account defect structure, time, and gradients in stress, temperature and composition.

The report also proposes an experimental program based on the refined helium embrittlement model. A parametric study of the effect of initial defect density on the resulting helium bubble distribution and weldability of tritium aged material is proposed to demonstrate the roll that defects play in embrittlement. This study should include samples charged using vastly different aging times to obtain equivalent helium contents. Additionally, studies to establish the minimal sample thickness and size are needed for extrapolation to real structural materials. The results of these studies should provide a technical basis for the use of tritium aged materials to predict the weldability of irradiated structures. Use of tritium charged and aged material would provide a cost effective approach to developing weld repair techniques for ITER components.

TABLE OF CONTENTS

	<u>Page No.</u>
ABSTRACT*	1
TABLE OF CONTENTS*	2
TASK SPECIFICATIONS*	3
WORK PLAN/PROCEDURE/METHOD*	3
EXPLANATION/DISCUSSION OF ACTIVITIES*	4
Introduction	4
Collection And Analysis of Pertinent Data	4
General Observations on Helium in Metals	7
Bubble Size and Stability	7
Role of Microstructure	8
Role of Helium Content	10
Role of Temperature and Time	11
Role of Stress and Stress Gradients	12
A Refined and Simplified Helium Embrittlement Model	13
Suggestions for Future Work	15
RELEVANCE FOR THE ITER DESIGN*	16
VERIFICATION AND VALIDATION	17
REFERENCES*	18
FIGURES	
1. Size Frequency Distribution of Helium Bubbles	21
2. Helium Bubble Nucleation Sites	22
3. Helium Bubble Distribution Near a Grain Boundary	23
4. Effect of Prior Cold Work on Swelling	24
5. Effect of Neutron Fluence on Swelling	25
6. Comparison of Weld Heat Affected Zone Cracking	26
7. Effect of Helium Content on Reduction in Area	27
8. Effect of Helium content on Creep Rupture	28
9. Strain Rate Dependence of Ductility	29
10. Time Dependence of Bubble Growth	30
11. Temperature Dependence of Tensile Ductility	31
12. Helium Bubble Development on Grain Boundaries	32
13. Illustration of Variables Effecting Degradation Processes	33
14. Influence of Variables Swelling, Creep, and Weldability	34

TASK SPECIFICATIONS

This report is in fulfillment of Task Agreement G15TT1296-05-15FU (Vacuum Vessel Section Models, Blanket Support Structures, and Welding, Cutting, and Inspection Development for the VV and Blanket (T204-9)); Subtask 5 (Welding Comparison of Irradiated and Tritium Charged SS); Phase 1 (Sample Preparation and Testing); Part 1 (Develop Plan to Define Differences Due to Helium Implantation Methods).

Work specification: Collection and analysis of pertinent data will lead to an improved understanding of the helium embrittlement process and a refined model. The latter will serve to define the work required to explain the differences observed between welding on irradiated and tritium charged & aged SS and to focus future work needed to make successful weld repairs of ITER components.

WORK PLAN/PROCEDURE/METHOD

The initial step to formulate a refined model for the helium embrittlement process and to determine a focus for future work involved a detailed review of the literature on helium embrittlement effects. This survey included not only reports on weldability of irradiated stainless steel, but the large volume of reports on effects of irradiation on material properties including atomistic theories for embrittlement. Selected reports are listed in the Reference Section and are discussed in the body of the report.

Selected ideas from the literature were pulled together as they pertain to a model for the helium embrittlement observed during welding of irradiated stainless steels. Bubble size and stability, microstructure, helium content, temperature, and stress all effect embrittlement. These factors are discussed in the section on General Observations on Helium in Metals.

Ideas from the literature, combined with experience at Savannah River, led to the development of a refined model for helium effects on weldability, consistent with available data. This unique model is described in the Section "A Refined and Simplified Helium Embrittlement Model".

This literature review and helium embrittlement model provide a focus for future work to meet the needs of ITER. This focus, and suggestions for individual experiments, are discussed in the section on "Suggestions for Future Work".

EXPLANATION/DISCUSSION OF ACTIVITIES

Introduction

Stainless steel is a candidate structural material for use in fusion reactors, high energy accelerators, and other emerging applications. Repair and/or replacement of components that experienced service related degradation will have significant impact on both system design and maintenance schedules. Many of these components will experience helium implantation or build-up during service. Additionally, many fission reactor components now in need of repair have experienced helium build-in. Helium accumulation will adversely impact the weldability of the steel, thus increasing the difficulty of weld repair and/or increasing the down time associated with any weld repair process. The effects of helium on weldability and the suitability of any specific weld repair process can be evaluated either by welding on irradiated steels or by welding on steels which have had experienced helium accumulations through tritium decay ("tritium tricked" materials). These two helium implantation processes have vastly different impacts on the metallurgical condition of the steel and perhaps on the helium distribution in the steel. Either or both of these differences could impact the effects of helium on weldability and minimize or eliminate the relevance of less costly work with tritium tricked materials to materials exposed to high energy irradiations. The analyses presented in this work evaluated this potential difference by modeling the metallurgical process that causes the helium induced degradation in weldability and relating the model to other helium induced degradation processes.

Collection and Analysis of Pertinent Data

The weldability of irradiated austenitic stainless steels is significantly less than that of non-irradiated steels because of the build-in of helium during irradiation. Helium induced reductions in weldability were first reported in 1978, when thin (0.51 mm) walled, irradiated, Type 304 L stainless steel tubing was shown to develop occasional "grain boundary separations at the tube inner diameters near the weld zone" during inert gas-tungsten arc welding procedures¹. The weld heat affected zone cracking was attributed to helium embrittlement caused by grain boundary precipitation of helium bubbles. However, in spite of the occasional cracks, this early work concluded that "tubing having fast flux exposures as high as 7.51×10^{22} n/cm² may be successfully welded using conventional GTAW fusion welding procedures"¹.

The real impact of the helium on weldability of irradiated stainless steels became apparent when heat affected zone (weld toe) cracking prevented the repair of a stress corrosion crack in the wall (12.7 mm thick) of a nuclear reactor tank². The Type 304 stainless steel tank wall contained approximately 3 appm He in the stress corrosion cracked region. Efforts to weld a patch over the stress corrosion cracks caused intergranular, weld heat affected zone cracks in the tank wall. These HAZ cracks were deep, apparently interconnected and caused leaks in the tank wall². Subsequent, laboratory studies confirmed the adverse effects of helium on the weldability of stainless steels and demonstrated that special, and somewhat restrictive welding procedures were necessary to produce successful (minimal cracking) welds on helium containing stainless steels³⁻⁹. These welding studies also demonstrated that a significant amount of intergranular HAZ cracking accompanied the conventional welding of austenitic stainless steels containing as little as one appm helium. The cracked samples showed very little evidence of macroscopic plastic deformation and transmission electron microscopy studies of the near weld regions suggested that a weld overlay process which caused only 1 - 2% plastic strain¹⁰, could cause helium induced cracking in helium charged samples^{3,7,9}. Cracking was attributed to the coalescence of helium bubbles along grain boundaries. Such observations are consistent with the use of the term "helium embrittlement" to describe the observed reductions in weldability.

High temperature helium embrittlement is also apparent from tensile data for both tritium charged^{11,12} and irradiated^{13,14} austenitic alloys. The combined tensile data demonstrate that helium build-in has a minimal effect on the room temperature tensile ductility of irradiated alloys^{13,14} until the helium concentration approaches 700 to 800 appm¹⁵. At those higher helium levels, the ductility was significantly reduced. Additionally, significant reductions in tensile ductility are apparent in both the irradiated and the tritium charged samples tested at temperatures above 773 to 873 K. The level of the helium induced reduction in ductility was dependent on helium content, helium implantation technique, test temperature, metallurgical condition, test strain rate, alloy chemistry and other material/process variables. The importance of helium implantation technique on tendency toward embrittlement is attributed to the displacement damage associated with irradiation and the lack of displacement damage in tritium charged materials. In general, embrittlement is promoted by increasing the test temperature, decreasing the strain rate and increasing the helium content. The embrittling effects of helium on the tensile properties of austenitic steels are similar to the helium induced reductions in weldability and are associated with the nucleation and coalescence of helium bubbles along grain boundaries and other metallurgical interfaces. Helium bubble formation also plays a major role in the nucleation of irradiation induced swelling of metals and alloys; however, the temperature range for the onset of high temperature helium embrittlement of austenitic steels is slightly higher than the 673 K range reported for the onset of void swelling.

Swelling during the irradiation of austenitic stainless steels generally initiates when the displacement levels approach 40 to 50 displacements per atom¹³. This corresponds to a helium content of several hundred appm. The specific helium content is dependent on the irradiation spectrum and the displacement damage necessary to cause swelling initiation is dependent on the metallurgical condition of the steel. High rates of helium build-in reduce the displacement level for the onset of swelling while cold work and other metallurgical changes that increase the number of helium bubble nucleation sites, decrease the average size of a helium bubble for any given helium content and suppress the onset of swelling¹⁶. Such observations suggest that the development of a critical, or stable, helium bubble size is critical to the initiation of swelling processes¹⁷. This observation provides the basis for the design of a swelling resistant alloy by increasing the number and depth of helium traps in the lattice by increasing the density of chemical and mechanical defects.

Swelling in austenitic stainless steels is near a maximum when the temperature is in the range of 725 to 850 K¹⁶. This critical temperature range corresponds to the temperature range for weld HAZ cracking and to the onset of large scale ductility losses during tensile tests of helium containing austenitic materials. The degradation processes involved in swelling, loss of tensile ductility and loss of weldability are similar and include the nucleation, growth and/or coalescence of helium bubbles or microvoids. Creep and creep rupture also involve void nucleation and growth and, in that respect, helium effects on creep behavior should mimic helium effects on the weldability of austenitic steels.

The presence of helium reduces the strain and time to rupture in a creep test¹³. Simplified models of the rupture process show that the low failure strains result from the nucleation of closely spaced cavities at grain boundaries and that, for a given applied stress, the time to failure reduces as the grain size increases¹⁸. Bubble growth is enhanced by normal tensile stresses; thus, grain boundaries oriented normal to the creep stress axis develop particularly large bubbles which subsequently coalesce and produce fracture^{16, 18}. These, and numerous other observations, provide a technical basis to model the development of heat affected zone cracking during welding of helium containing materials. Additionally, review of the literature provides a basis to conclude that the method of helium introduction may significantly influence the level of damage associated with any given welding process.

General Observations on Helium in Metals

Bubble Size and Stability

Many of the various deleterious effects of helium on the mechanical properties of metals and alloys are associated with the nucleation, growth and coalescence of bubbles on grain boundaries. The very limited solid solubility of helium in most crystalline metal structures basically dictates that most of the helium implanted in a metal lattice is "dissolved" as a supersaturated solid solution. Given time and the thermal energy necessary for motion, the "dissolved" helium atoms will diffuse and gather into small (0.5 to 1nm) clusters. The clusters, or bubble nuclei, will either grow or dissolve, depending on the rate of arrival and departure of helium atoms and vacancies. The nuclei becomes stable when a critical size, or radius, is achieved. This critical radius is typically a few nanometers¹⁷. The size of this critical radius is reduced for heterogeneous nucleation processes such as precipitation on grain boundaries and dislocations. The helium gas pressure, p_g , exerted by n atoms inside the bubble of radius r , is given by:

$$p_g = nkT/(4\pi r^3/3 - nb_v)$$

where b_v is the Van der Waal's constant for helium¹⁹. Thus, the helium pressure in small bubbles will be typically higher than in large bubbles and, because the lattice concentration of helium in local equilibrium with the bubble is directly proportional to p_g (helium is a monatomic gas), the ease of helium relocation from "stable" bubbles will be approximately proportional to $1/r_3$. This observation, coupled with the observation that the stable bubble size is a few nanometers, provides a basis to conclude that, given the thermomechanical events associated with welding, bubble coalescence will be more rapid in irradiated samples than in samples that were tritium tricked.

The typical bubble radius in austenitic stainless steels containing helium that was introduced through tritium decay is 1 to 2 nm^{5,10}. This bubble size is roughly equivalent to the "few nanometers" size required for formation of a stable helium bubble and suggests that the tritium trick process (tritium charging, aging and tritium offgassing) produces a population of stable helium bubbles. This conclusion is supported by observations which demonstrate that, although the mean bubble size increases with the annealing time at 1373 K, there is no significant decrease in the number of very small bubbles²⁰. Data demonstrating the stability of the small bubbles is shown in Figure 1.

The helium bubble microstructure in a tritium tricked sample is apparently dependent on the metallurgical condition of the material. Grain boundary bubbles about 1.8 to 2.0 nm in diameter were apparent in Type 316 specimens that contained 0.18 appm He after tritium charging at 573 K for 30 days and

detritiation by vacuum offgassing at 673 K⁵, while no bubbles were found in tritium tricked Type 316L samples containing 50 appm He after tritium charging at 723 K for 6 hours, storing (aging) at 243 K for one year and detritiation by vacuum offgassing at 723 K for 300 hours²¹. The samples containing helium bubbles had been fully annealed (one hour at 1323 K) prior to tritium charging while the samples that did not contain bubbles, in spite of the higher helium content, had apparently been tritium charged in an as-received, mill annealed, condition. The fully annealed samples contain fewer sites for the nucleation of helium clusters and/or bubbles. The lack of helium trapping sites (defects) in the fully annealed microstructure increases both the apparent diffusivity of helium and the average distance that a helium atom must migrate before encountering a potential nucleation site. The potential for such microstructural effects had been recognized²¹; however, the lack of helium bubbles was attributed to shorter time of tritium charging.

Role of Microstructure

Grain boundaries, dislocations and other crystalline defects play major roles in the nucleation and growth of second phase precipitates in crystalline solids. The interfaces associated with such defects serve as low energy sites for second phase nucleation and form high diffusivity paths for the atom migration necessary to accommodate the compositional changes that generally accompany precipitation. Additionally, moving dislocations can drag solute atmospheres, including precipitate nuclei and small bubbles, thus enhancing precipitate growth and coalescence processes. These effects combine to favor the nucleation of precipitates on crystalline defects and the growth of precipitates on large internal interfaces such as grain boundaries.

Helium bubbles in annealed, tritium tricked, austenitic stainless steel samples nucleate on grain boundaries (Figure 2a), dislocations (Figure 2b), carbide-matrix interfaces (Figure 2c) and within the metal lattice (Figure 2d). Bubble precipitation within the lattice is often accompanied by the punching of dislocation loops, as illustrated in Figure 2d. The importance of microstructure to the precipitation process is apparent when the bubbles develop on obvious defects. This role is not as apparent when precipitates develop within the metal lattice. However, helium trapping by vacancies is well established and calculations of bubble development within the lattice have been associated with such trapping¹⁹. The bubble denuded zones, apparently associated with near grain boundary vacancy concentration gradients, were found in tritium tricked, austenitic stainless steels (Figure 3). The general size of the helium bubbles in these tritium tricked samples, 2 to 4 nm diameter, is consistent with a critical radius of approximately one nanometer. These observations are also consistent with the majority of the observations with tritium tricked samples (References 4, 5 and 10, for example). The collective observations demonstrate that in fully annealed, tritium tricked samples, stable helium bubbles precipitate on grain

boundaries when as little as 0.18 appm He is introduced. Increasing the helium concentration causes bubble precipitation on dislocations, carbide particles and vacancies. Bubble development was apparently inhibited if the samples were not fully annealed prior to the tritium tricking process. This inhibition is attributed to an increased defect density in the as-received samples. The increase in defects represents an increase in the number of helium traps in the metal lattice and an increased difficulty for sufficient helium migration to support the development of a critical radius. Support for this conclusion is apparent in other literature describing helium effects in materials.

Prior cold work suppresses helium bubble growth in palladium containing up to 50 appm helium²¹. The increased dislocation density associated with cold work increases the number of bubble nucleation sites. This increase in bubble density decreases the size of the average bubble, increases the equilibrium helium pressure inside the bubble, [$p_g = f(1/r^3)$], and decreases the tendency for bubble growth. Prior cold work also suppresses irradiation induced swelling. The magnitude of this effect is related to the dislocation density and distribution and generally increases as the amount of cold work increases (Figure 4)¹⁶. The helium-defect interactions to the swelling resistance of metals and alloys is relatively well established and has been used to provide a theoretical basis to recommend the design of swelling resistant alloys²³. This theory is based on the recognition that "a critical number of gas atoms are required in a cavity before point defect driven swelling can begin"²³. This recognition leads to the general, clearly simplified, conclusion that increasing the helium trap density by processes such as cold work and perhaps even irradiation will suppress swelling. The case for irradiation induced defects suppressing swelling is apparent from the influence of displacement rate on swelling. Accelerated displacement rates shift the swelling threshold to higher temperatures (Figure 5) probably as a consequence of several rate dependent processes¹⁶. These processes include the precipitation and dissolution of second phases and the evolution of dislocation and loop substructure¹⁶.

The interaction of irradiation induced defects with helium has been summarized by concluding that soon after the onset of irradiation the displacement induced vacancies and interstitials reach a stationary concentration. The concentration of He atoms, however, increases with time. During the early stages of irradiation, the He concentration is too low for significant clustering and bubble nucleation is negligibly small. With increasing He concentration (irradiation) clustering increases and deep helium traps are introduced¹³. Eventually, the number of helium atoms at the trap sites reaches the level necessary to cause bubble nucleation. The bulk He concentration required for bubble nucleation will depend on the number of trap sites. High displacement rates (high fluence) will increase the stationary vacancy and interstitial concentrations and prior cold work will increase the dislocation density in the material. Point defects and dislocations are effective trap sites for He atoms, thus increasing either the level

of prior cold work or the displacement rate will increase the number of helium clusters and suppress the onset of swelling as shown in Figures 4 and 5.

A generalization of the above observations is that, for a given helium concentration, fewer stable helium bubbles will develop during the helium implantation process with an increase in defect density. A corollary to this generalization is that amount of helium readily available for relocation increases as the defect density increases because the relocation of He atoms from stable bubbles is more difficult than the relocation of helium from metastable nuclei. This corollary observation, coupled with the conclusion that the displacement damage associated with irradiation increases the density of effective helium traps, suggests that, for a given helium content, helium bubble coarsening and coalescence will be suppressed in fully annealed, tritium tricked material relative to irradiated samples of the same material. Such suppression would suggest that irradiated samples will be more difficult to weld than tritium tricked samples with similar helium contents. Direct comparisons of the effect of helium implantation technique on the weldability of Type 304 stainless steel confirm this conclusion and demonstrate that for the conditions tested, weld heat affected zone cracking in irradiated materials are 25 to 30 greater than in tritium tricked materials welded by the same processes (Figure 6)²⁴.

Role of Helium Content

The adverse effects of helium on the mechanical properties and weldability of austenitic stainless steels increases as the helium content increases: Tensile tests of tritium tricked Type 316LN stainless steel demonstrated that increasing the helium content from 0 to 432 appm decreased the reduction in area at fracture from 97 to approximately 15 % for tests at 1043 K (Figure 7a)¹². Similar behavior was noted in tests to determine the effect of helium on weld heat affected zone cracking in Type 304 stainless steel samples that had been welded by a low penetration overlay welding process (Figure 7b)³. These observations are consistent with the increased tendency for HAZ cracking in Type 304 samples that were tritium tricked to increasing helium levels³.

Creep and stress rupture testing of helium containing materials also demonstrate that the extent of property degradation is dependent on the helium content. Helium effects on the creep behavior have been observed in samples containing less than one appm He. The influence of helium content on creep rupture time and the strain to rupture in a Type 316 austenitic stainless steel are summarized in Figure 8¹³. The influence of helium on the creep behavior increases as the helium implantation rate decreases, and are higher for "in-pile" tests than for post irradiation tests of comparable materials¹³. The creep rupture fracture morphology is consistent with that observed in high temperature tensile tests and weld heat effected zone cracking of helium containing materials;

intergranular with many, but not all, of the grain boundary facets showing a relatively uniform distribution of dimples.

The loss in elevated tensile and creep ductility and the tendency for weld heat affected zone cracking are attributed to the growth and coalescence of microvoids which initiated at helium bubbles present on the grain boundaries. During welding of helium containing materials, these grain boundary bubbles serve as initiation sites for the microvoids which grow and coalesce under action of the thermo-mechanical forces present during the welding operation. These forces provide the thermal energy necessary for vacancy migration and redistribution of helium-point defect clusters and for the accumulation of both vacancies and helium atoms in the microvoid nuclei. The nature of the bubble/void growth during any given welding operation will depend on the availability of both vacancies and helium atoms, the bubble density prior to welding and the bubble nucleation rate during the welding operation. These observations suggest that higher helium contents will increase extent of weld heat affected zone cracking by:

- a) increasing the density of intergranular helium bubble sites, and
- b) increasing the amount of helium available for redistribution.

However, both of these quantities are dependent on the microstructure of the helium containing material and the technique and conditions used to introduce helium to the metal lattice.

Role of Temperature and Time

The effects of helium on swelling, creep, elevated temperature tensile behavior and the weldability of metals and alloys are consistent with a microstructural evolution that is dependent on helium atom mobility. Single atoms move through the metal lattice until they are trapped at microstructural defects, including grain boundaries, dislocations, vacancies and interstitials. The mobility of the "trapped" atoms is dependent on the trap depth and when that depth is sufficient the first atom trapped may be in residence at the trap site when a second or third atom arrives and a helium atom cluster is formed. The depth of the trap is likely to increase with cluster formation thus increasing the residence time of the collected atoms. The clusters will grow as additional helium atoms are collected and when the cluster reaches a critical size a stable helium bubble is formed. This microstructural evolution process is diffusion controlled. Additionally, the growth of helium bubbles, whether by the accumulation of helium atoms or vacancies is also diffusion controlled. Diffusion and trapping are both thermally activated processes. Increasing the temperature increases the mobility of the helium atoms, vacancies and helium-vacancy clusters. Furthermore, increasing the temperature increases the thermal energy available for detrapping.

The impact of helium on bulk materials properties is generally attributed to the kinetics of intergranular cavity growth^{4,13} and the ability of helium to influence the nucleation and/or growth of the cavities. Because helium mobility is controlled by diffusion and trapping processes, the adverse effects of helium will generally increase with increasing temperatures and with increasing time at temperature.

The effect of time is apparent from the strain rate dependence of helium embrittlement in a stainless steel that contained 7 appm helium and tested at 823 K (Figure 9)¹³. Little or no effect was apparent when the irradiated steel was tested at strain rates above 10^{-2} and the magnitude of the embrittlement increased with decreasing strain rate for all rates tested below 10^{-2} . These tensile data are consistent with 873 K fatigue data for Type 316 stainless steel containing 800 appm, except that fatigue studies demonstrate helium effect at higher strain rates. However, the observation of effects at higher strain rates is consistent the anticipated effects of increased helium content and test temperature.

Helium bubble development is also dependent on time at temperature. The average size of a helium bubble, in non-stressed material, increases with the square root of time (Figure 10), as anticipated for a diffusion controlled process²⁵. The importance of diffusion is also apparent in tensile tests of tritium tricked samples. The reduction in area of tritium tricked, Type 316 stainless steel was not impacted by 432 appm helium until the temperature reached approximately 673 K and helium became mobile in the steel lattice (Figure 11)¹². This temperature threshold is relatively consistent with the general observation that vacancies are significantly mobile when the temperature is approximately 0.4 times the melting temperature. The magnitude of helium embrittlement in a tensile test increases with increasing the test temperature because of the increasing helium mobility.

Role of Stress and Stress Gradients

Stress plays a major role in helium embrittlement processes because:

- a) stresses in excess of the flow stress for the material will cause dislocation motion (Dislocation dragging of helium atmospheres and/or helium bubbles has been associated with dislocation motion, Reference 21 for example, and such dragging promotes the relocation of helium.),
- b) the dislocation motion, per se, will generate vacancies throughout the metal lattice and dislocation-bubble interactions will promote bubble growth, and
- c) bubble coarsening will be favored in grain boundaries oriented perpendicular to tensile stresses.

Additionally, most measures of helium induced degradation involve the application of a stress, thus an involvement of stress with the embrittlement is unavoidable.

A schematic diagram illustrating the influence of stress on grain boundary cavity development (Figure 12) suggests that coarsening is sensitive to the stress acting on the material. The effect of stresses on the orientation of phases has been known for decades and early work on stress orientation of hydrides in zirconium based alloys demonstrated that when hydride precipitation occurs in a stressed sample, most of the hydride platelets were oriented perpendicular to tensile stresses and parallel to compressive stresses²⁶. The tendency toward stress orientation caused hydride embrittlement to be much more severe than would be anticipated in materials that contained unoriented hydrides. Recent theoretical studies of precipitate clustering²⁷ demonstrated that precipitates develop strong spatial correlations to align in specific orientations and, because of this alignment, a group of individual precipitates may coarsen as an entity. This generalized observation is consistent with the observed tendency for large helium bubbles to be preferentially located on bubbles perpendicular to an applied tensile stress¹³, and for the success of stress modified welding processes that altered the evolution of helium bubbles such that bubbles occurred predominately on grain boundaries perpendicular to the weld direction²⁸.

Stress and temperature gradients also impact helium bubble development. Inert gas bubbles have been observed to migrate in thermal gradients because of the strong interaction between the bubble and the flux of diffusing atoms. However, the vacancy flux associated with the diffusing atoms is not sufficient to cause the observed bubble migration and a role for a temperature or stress gradient must be invoked²⁹. Welding processes produce large thermal and stress gradients. These gradients, which are dependent on the welding process may play major roles in the coarsening of helium bubbles.

A Refined and Simplified Helium Embrittlement Model

A model for helium embrittlement must take into account the following experimental observations:

- An increase in helium cracking with an increase in helium concentration
- Helium cracking is dependent on both elevated temperature and the presence of a tensile stress
- Helium bubbles in annealed material are:
 - Within grains, with higher concentrations along grain boundaries
 - Consistently about 3 nm diameter
- Helium bubbles grow due to the presence of heat and stress from a weld bead
- At fracture, helium embrittlement cavities are consistently 1 micron in diameter

- Zones "denuded" of helium bubbles appear next to some incoherent grain boundaries.

Helium embrittlement of a metal or alloy therefore involves the interaction of several variables including: helium content, temperature and stress. The specific nature of the interactions is influenced by other variables such as the metallurgical condition of the alloy, gradients in the alloy and time. For any given set of conditions, the metal-variable interactions may be represented by three circles. The individual circles represent temperature, helium content and stress respectively. Increasing temperature, helium level and stress are represented by circles of increasing radius. The interactions of two circles will represent the combination of variables necessary to cause a specific degradation event to occur in the material (e.g. the combination of stress and temperature necessary for creep, the combination of temperature and helium content necessary for swelling and the combination of stress and helium level necessary to stress oriented coarsening of helium bubbles along grain boundaries oriented perpendicular to the stress axis). The relative positions of the circles is determined by the microstructure of the helium containing material, the gradients acting on the material and the time at temperature. For modeling purposes, the position of the helium circle is controlled by the microstructure, the position of the temperature by time and the position of the stress circle by gradients in the material, Figure 13.

A pictorial representation of the degradation processes is illustrated in Figure 14 where the circles are shown to overlap. The central portion of the figure represents the combination of variables that cause heat affected zone cracking during the welding of a helium containing material. The importance of the variables is recognized by noting that weld cracking could be eliminated by changing: a) the size of the helium circle (reducing helium content), the position of the helium circle (altering the microstructure of the material), the size of the stress circle (placing a compressive stress on the weld joint during welding), the nature of the gradients (using low heat input welding processes), by reducing the time at temperature during welding (increasing the weld speed for a given heat input) and by reducing the temperature (using non-fusion welding practices). Each of these techniques has been used to improve the weldability of helium containing steels.

Acceptance that the weldability of helium containing materials involves the complex interaction of six or more variables may be the first step toward developing practical solutions to the welding problem even though the complexity of the helium embrittlement process has been widely recognized. For example, the importance of helium introduction parameters, test temperatures, strain rate and microstructure were emphasized in a 1986 review of helium effects on the properties of metals and alloys¹³. However, conclusions about the weldability of irradiated steels have been drawn from data with tritium tricked

materials with little reference to the importance of helium introduction technique and the resulting microstructure^{2-5,8}.

This refined model is consistent with most of the experimental data for helium effects on metals and alloys. However, as presented, the variables are shown to be relatively independent. Clearly, microstructure could effect the position of temperature circle as well as helium circle because the degree of cold work does impact the recrystallization temperature of most metals. Additionally only six variables are illustrated in the model. Other variables might be included in the model by invoking a rotation to the gradient, time and microstructure lines. However, the six variables used were selected because experimental and theoretical evidence clearly demonstrates the importance of these variables to the helium embrittlement process. Furthermore, reference to these six variables provides a basis to suggest further work to better define and evaluate the effect of helium implantation on the weldability of metals and alloys.

Suggestions for Future Work

The conclusion that irradiated samples are more susceptible to helium induced reductions in weldability than are well annealed, tritium tricked samples has several implications to future needs. The use of tritium tricked samples, rather than irradiated samples, as weldability test materials will reduce the cost of weld development studies. However, the tritium tricked materials must be made to simulate irradiated materials. The model suggests that increasing the defect structure prior to helium introduction should increase the number of helium trap sites and thereby increase the utility of the test material. This observation suggests that a parametric study of the effect of initial defect density on the resulting helium bubble distribution in, and weldability of, tritium tricked material should be made. These studies would include variations in the helium content in the material and would than be correlated with selected weldability studies on irradiated materials. Additionally, because of the observed influences of implantation rate on swelling, the parametric study should include samples charged to the same helium level but having obtained that level with vastly different aging times (high tritium content equates to high implantation rate while a low tritium content would equate to a low implantation rate).

The studies with tritium tricked samples have demonstrated that constraint during welding has a significant impact on the weldability. This observation is consistent with stress and stress gradients playing key roles in the weldability of helium containing materials. These observations indicate that weldability studies with thin, unconstrained samples have little meaning for real structural applications. However, the tritium charging and aging of thin samples is quicker and can be done at lower temperatures than is practical for full size components. This suggests that studies are necessary to establish the minimal sample thickness and size necessary for useful extrapolation to real structural materials.

The data obtained during the programs outlined should provide a technical basis to use tritium tricked materials to predict the weldability of irradiated structures. However, until that information is obtained, the relevance of welding tritium tricked samples to either fission or fusion reactor applications is uncertain. Additionally, because of the multivariable influences on the effect of helium content on weldability, any specification of a minimal helium content for assured weldability must include a specification of the welding process, including the size and configuration of the component to be welded, and be related to the microstructure of the material.

RELEVANCE FOR THE ITER DESIGN

The International Thermonuclear Experimental Reactor (ITER) will require component replacement and repair during its operating lifetime. Replacement components will need to be reconnected to structures remaining in the reactor. Some of these structures will have accumulated helium in the metal lattice as a result of neutron irradiation and/or tritium exposure. Helium in 316L stainless steel (and other metals and alloys) can cause weld heat affected zone cracking, which may interfere with the ability to replace components and repair the reactor structure.

Experimental programs to determine the weldability of ITER materials of construction must rely on the availability of materials irradiated at ITER conditions, or on substitute materials. A primary and cost effective substitute for irradiated material is tritium charged and aged material. The tritium in this material decays to helium, thereby acting as a stand-in for irradiated material for the determination of weldability. This substitution has been shown to be qualitatively representative but quantitative differences are known to exist.

The model and experimental program developed in this task addresses these issues. The model provides a basis for understanding how stress, temperature, and helium content interact with time, defect structure and gradients. The experimental program will provide the additional data needed to support the applicability of test samples currently in use, namely tritium charged and aged stainless steel of various thicknesses.

VERIFICATION AND VALIDATION

The information in this report meets the deliverables in the Task Specifications. A refined helium embrittlement model, which fits available data, is presented. An experimental program to explain the difference observed between welding on irradiated and tritium charged and aged stainless steel is proposed.

REFERENCES

- 1) M. M. Hall, Jr., A. G. Hins, J. R. Summers and D. E. Walker, "Fusion Welding of Irradiated AISI Type 304L stainless Steel Tubing", Weldments: Physical Metallurgy and Failure Phenomena, Proceedings of the Fifth Bolton Landing Conference, Edited by: R. J. Christoffel, E. F. Nippes and H. D. Solomon, General Electric Company, Schenectady, NY, 1978, p. 365
- 2) W. R. Kanne, Jr., Welding Journal, Vol. 67 (8), 1988, p. 33
- 3) W. R. Kanne, Jr., G. J. Buck, A. Madeyski, D. A. Lohmeier, M. R. Louthan, Jr., D. T. Rankin, R. P. Shogan, G. G. Lessmann, and E. A. Franco-Ferreira, "Weld Repair of Helium Degraded Reactor Vessel Material", Proceedings of the Fifth International Symposium on Environmental Degradation of Materials in Nuclear Power Systems - Water Reactors, American Nuclear Society, Le Grange Park, IL, 1992, p. 390
- 4) S. H. Goods and N. Y. C. Yang, Metallurgical Transactions, Vol. 23A, 1992, p. 1021
- 5) H. T. Lin, M. L. Grossbeck and B. A. Chin, Metallurgical Transactions, Vol. 21A, 1990, p. 2585
- 6) W. R. Kanne, Jr., "Welding Tritium Exposed Stainless Steel", Hydrogen Effects in Materials, Edited by A. W. Thompson and N. R. Moody, The Minerals, Metals & Materials Society, 1996, p. 1057
- 7) W. R. Kanne, Jr., G. T. Chandler, E. A. Franco-Ferreira, D. T. Rankin, and M. R. Louthan, Jr., "Repair Welding of Irradiated 304 Stainless Steel", Maintenance and Repair Welding in Power Plants V, Conference Proceedings, American Welding Society and Electric Power Research Institute, 1994, p. 129
- 8) C. A. Wang, M. L. Grossbeck and B. A. Chin, Journal of Nuclear Materials, Vol. 225, 1995, p. 59
- 9) W. R. Kanne, D. A. Lohmeier, K. A. Dunn and M. H. Tosten, Materials Characterization, Vol. 30, 1993, p. 23
- 10) M. H. Tosten and P. A. Kestin, "Helium Bubble Distributions beneath GMA Weld Overlays in Type 304 Stainless Steel", Structure-Property Relationships and Correlations with the Environmental Degradation of Engineering Materials, Microstructural Science, Vol. 19., edited by D. A. Wheeler, G. W. E. Johnson, D. V. Miley and M. R. Louthan, Jr., ASM International, 1992, p. 3

- 11) M. R. Louthan, Jr., G. R. Caskey, Jr., D. E. Rawl, Jr. and C. W. Krapp, "Tritium Effects in Austenitic Steels", Irradiation Effects and Tritium Technology for Fusion Reactors, CONF-750989, Volume IV, Oak Ridge National Laboratory, 1976, p. 98
- 12) W. C. Mosley, "Effects of Internal Helium on Tensile Properties of Austenitic Stainless Steels and Related Alloys at 850°C", Hydrogen Effects in Materials, Edited by A. W. Thompson and N. R. Moody, TMS, 1996, p.855
- 13) H. Ullmaier, Nuclear Fusion, Vol. 24, 1984, p. 1039
- 14) M. L. Grossbeck and P. J. Maziasz, Journal of Nuclear Materials, Vol. 85-86, 1979, p. 883
- 15) A. J. West and D. E. Rawl, "Hydrogen in Stainless Steels: Isotopic Effects on Mechanical Properties", Tritium Technology in Fission, Fusion and Isotopic Applications, DOE CONF-800427, American Nuclear Society, 1980, p. 69
- 16) F. A. Garner, Materials Science and Technology, Vol. 10A, 1995, p. 419
- 17) L. K. Mansur, E. H. Lee, P. J. Maziasz and A. P. Rowcliffe, Journal of Nuclear Materials, Vol. 141-143, 1986, p. 633
- 18) R. M. Boothby, Journal of Nuclear Materials, Vol. 171, 1990, p. 215
- 19) M. Fell and S. M. Murphy, Journal of Nuclear Materials, Vol. 172, 1990, p. 1
- 20) A. Chanfreau, A. M. Brass, C. Haut and J. Chene, Metallurgical and Materials Transactions A, Vol. 25A, 1994, p. 2131
- 21) A. M. Brass, A. Chanfreau and J. Chene, Metallurgical and Materials Transactions A, Vol. 25A, 1994, p. 2117
- 22) R. Rajaraman, G. Amarendra, B. Viswanathan, C. S. Sundar and K. P. Gopinathan, Journal of Nuclear Materials, Vol. 231, 1996, p. 55
- 23) L. K. Mansur and E. H. Lee, Journal of Nuclear Materials, Vol. 179-181, 1991, p.105
- 24) W. R. Kanne, Jr., G. T. Chandler, D. Z. Nelson, and E. A. Franco-Ferreira, Journal of Nuclear Materials, Vol. 225, 1995, p.69
- 25) G. P. Tiwari and J. Singh, Journal of Nuclear Materials, Vol. 172, 1990, p. 114
- 26) R. P. Marshall and M. R. Louthan, Jr., Transactions of ASM, Vol. 56, 1963, p. 693

- 27) W. Hort and W. C. Johnson, Metallurgical and Materials Transactions A, Vol. 27A, 1966, p. 1461
- 28) C. A. Wang, H. T. Lin, M. L. Grossbeck and B. A. Chin, Journal of Nuclear Materials, Vol. 191-194, 1992, p. 696
- 29) G. P. Toward, Journal of Nuclear Materials, Vol. 232, 1996, p. 119

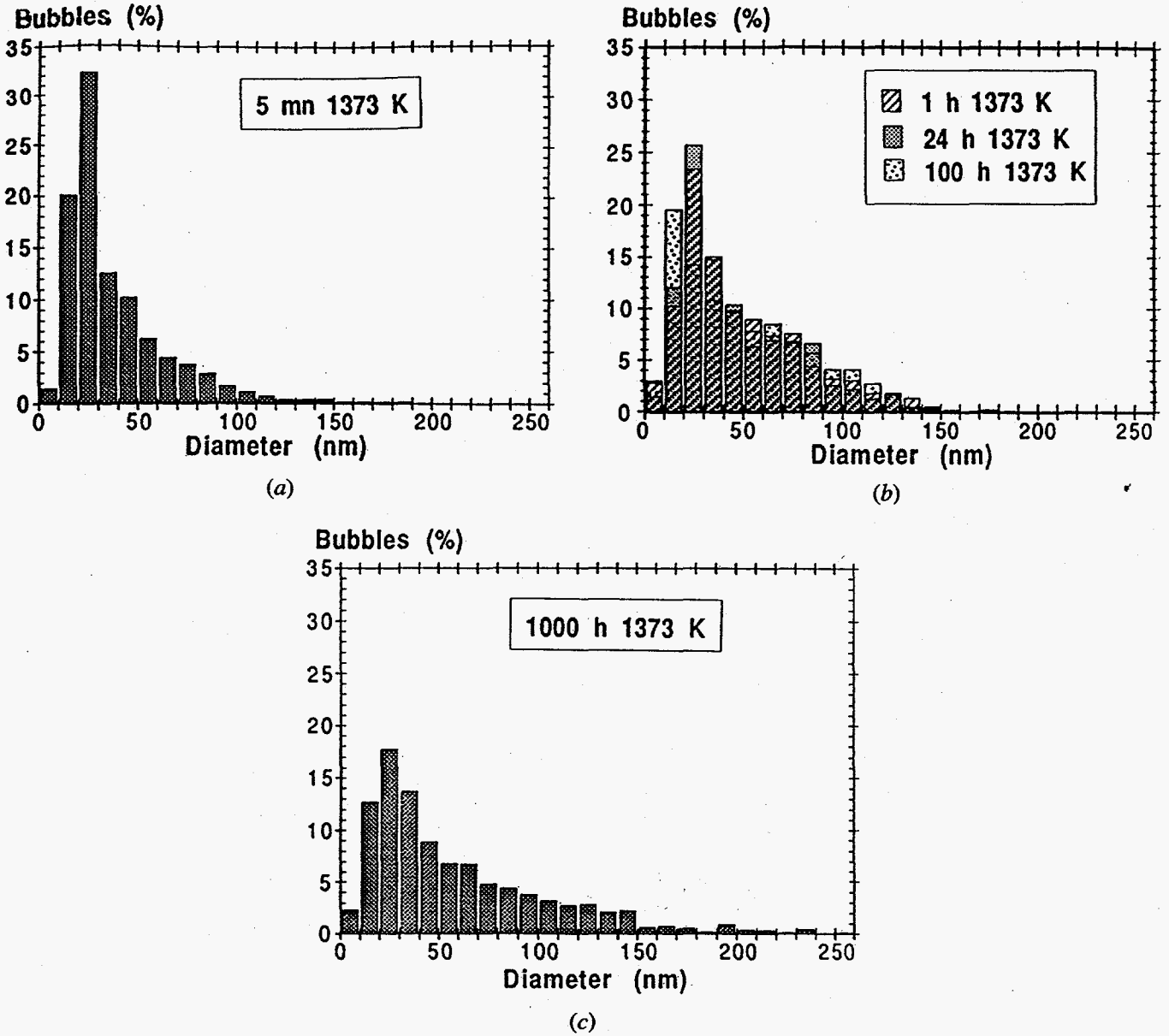


Figure 1. Size frequency distribution of helium bubbles in AISI Type 316L stainless steel samples that were charged with helium by the tritium trick method and then aged for various times at 1373 K. (After Reference 20)

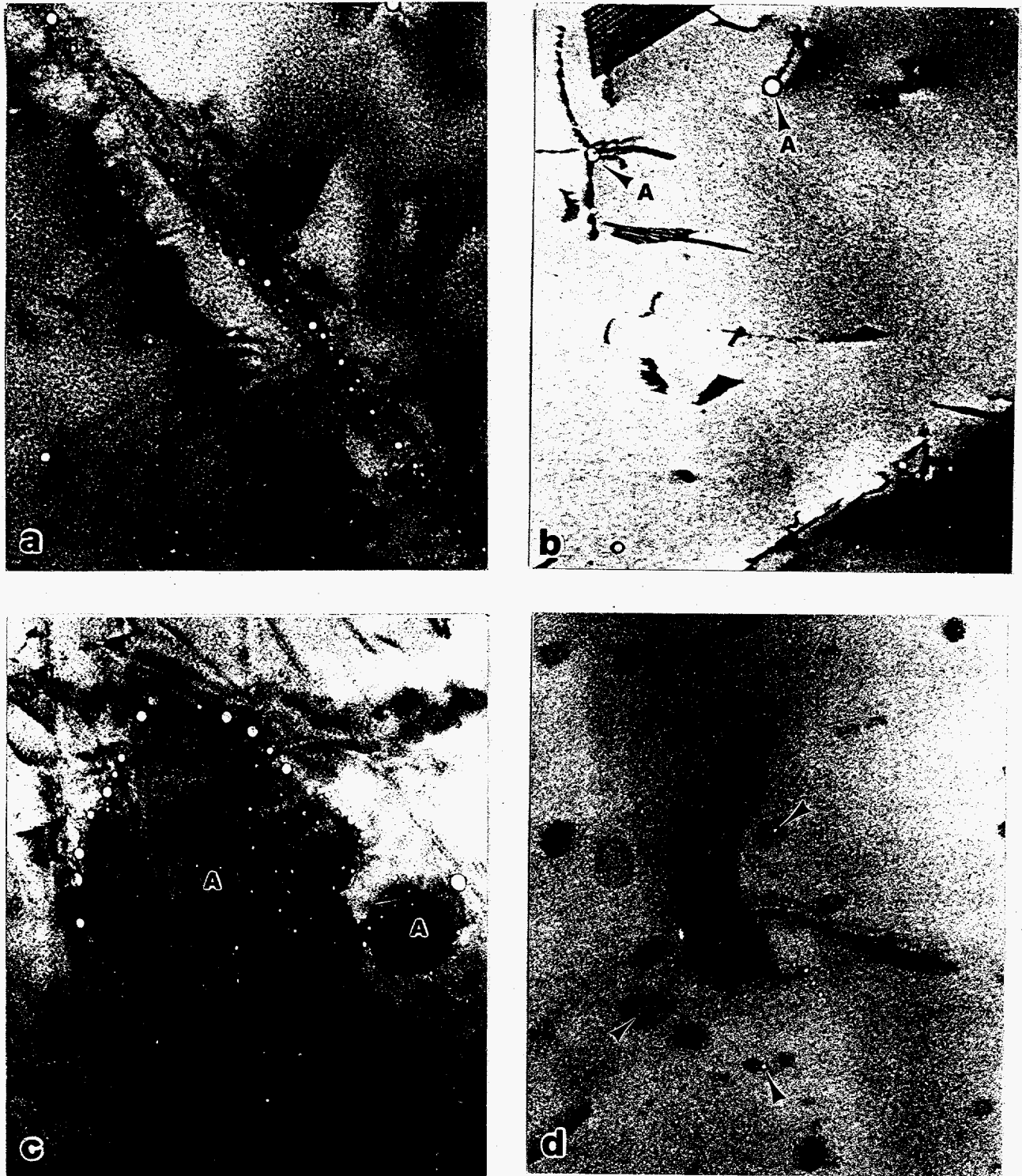
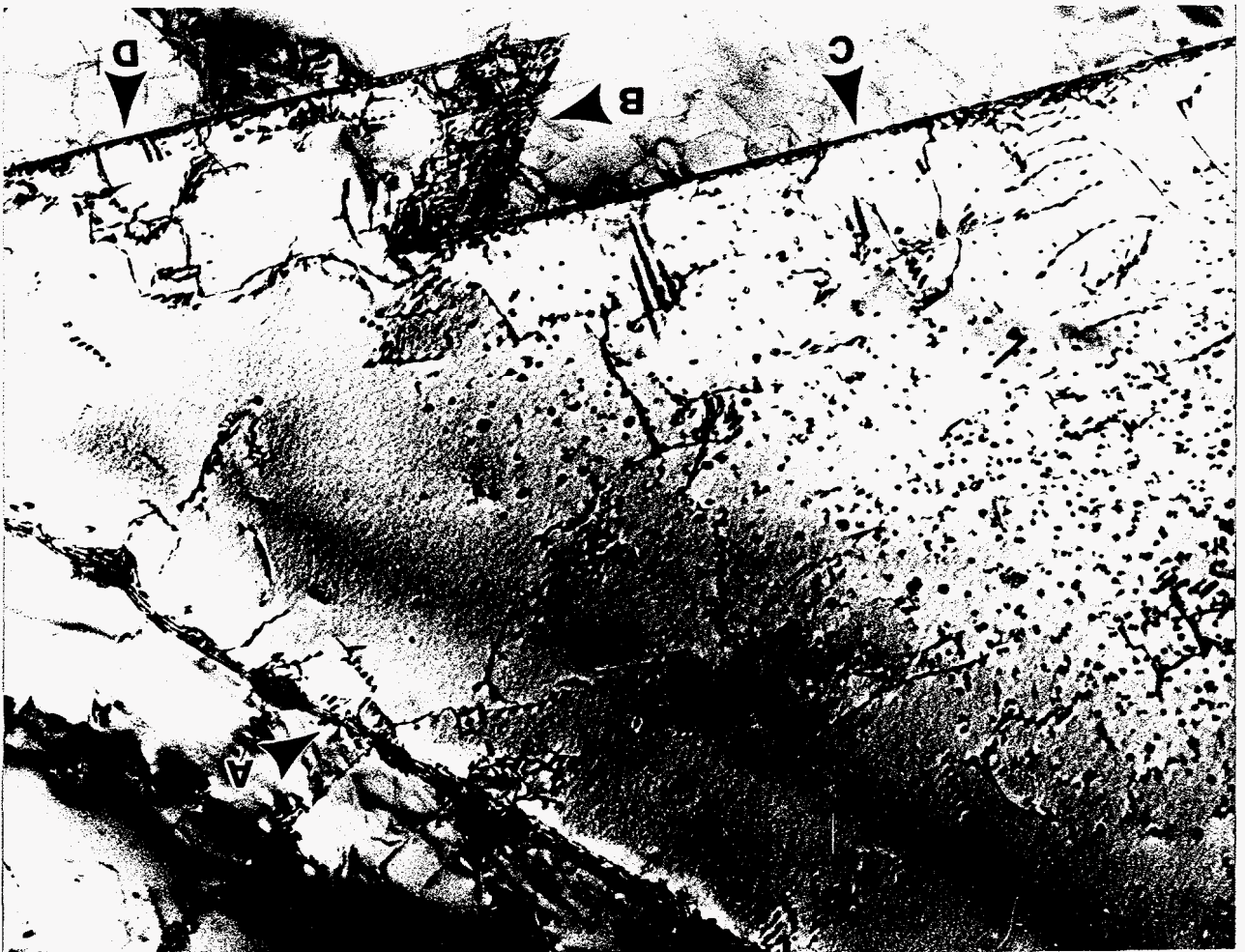


Figure 2. Typical helium bubble nucleation sites in fully annealed, tritium tricked, austenitic stainless steel. a) nucleation at high angle grain boundaries, b) nucleation at dislocations, c) nucleation at carbide-metal interfaces, d) nucleation within the austenitic grain.

Figure 3. Helium bubble distribution near a grain boundary in a tritium tricked austenitic stainless steel. Sample contained 147 appm He.



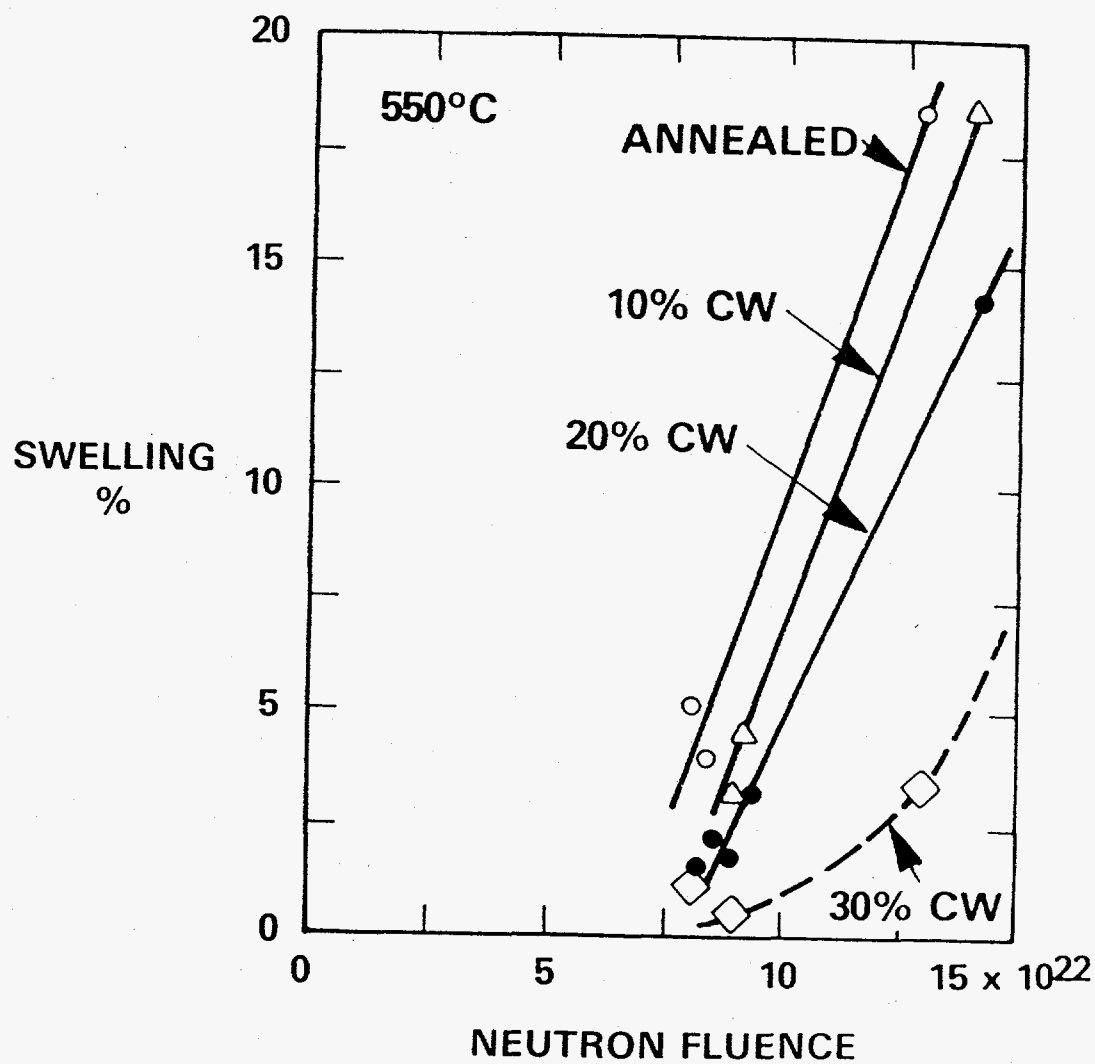


Figure 4. Effect of prior cold work on swelling of Type 316 stainless steel following irradiation at 823 K. (After Reference 16)

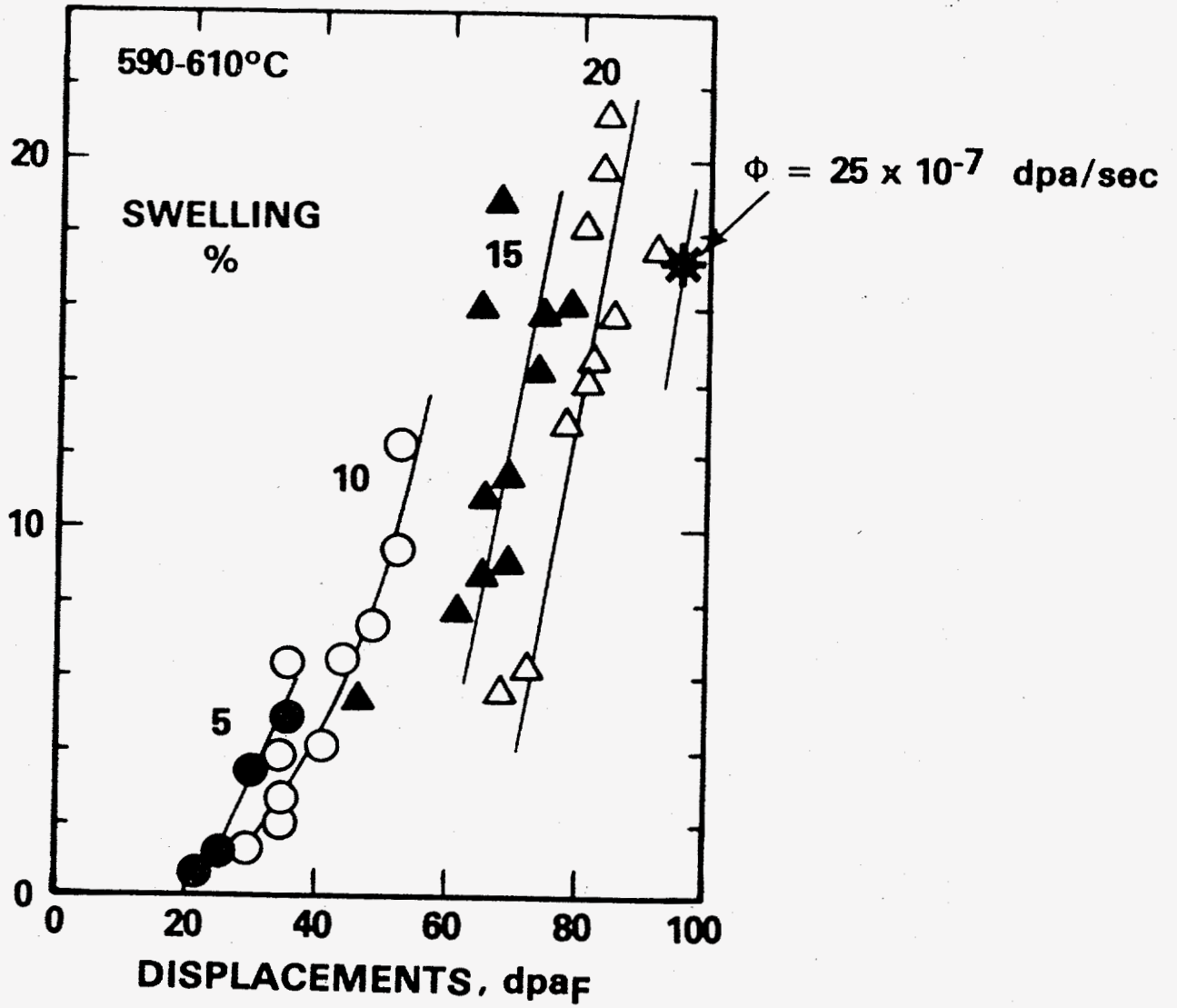
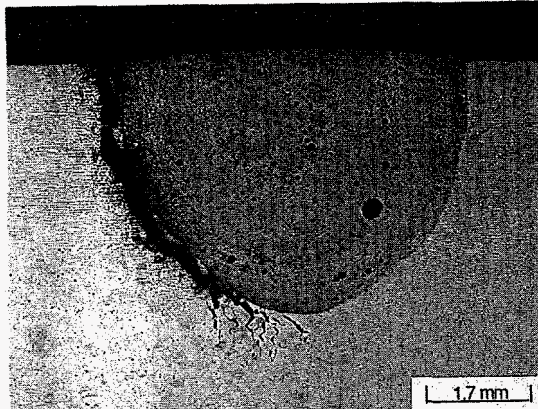
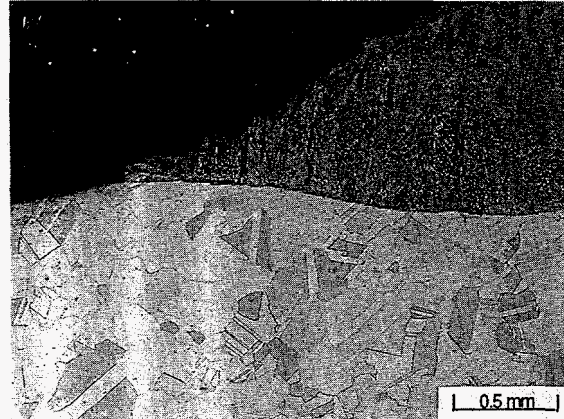


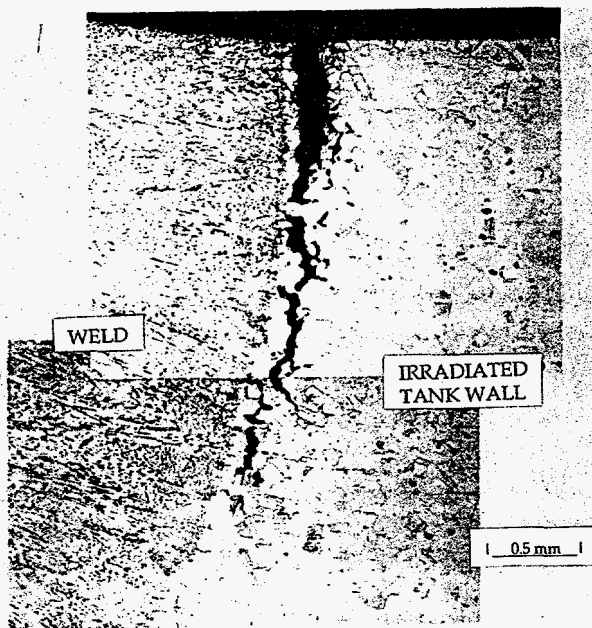
Figure 5. Effect of neutron fluence on swelling thresholds in Type 316 stainless steel. (After Reference 16)



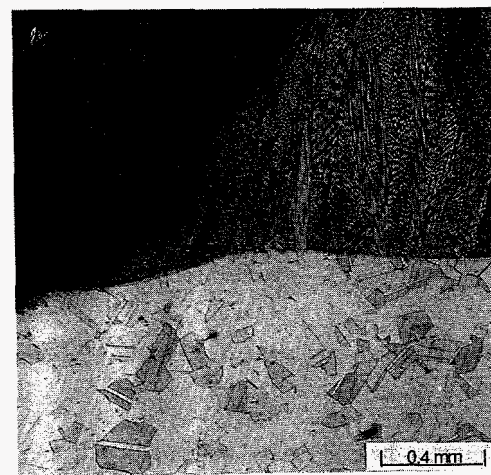
A. Tritium aged; Conventional
GTA Weld; 17 appm helium.



B. Tritium aged; Overlay weld;
17 appm helium.

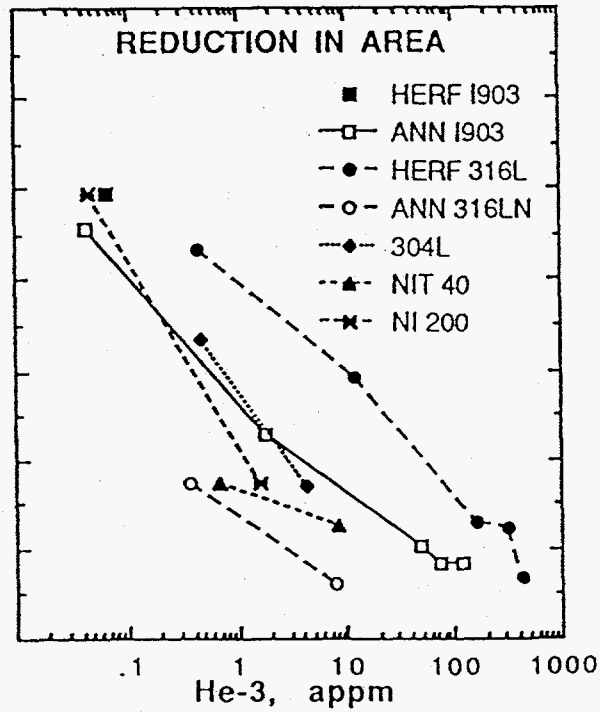


C. Irradiated; Conventional
GTA weld; 1.5 appm helium.

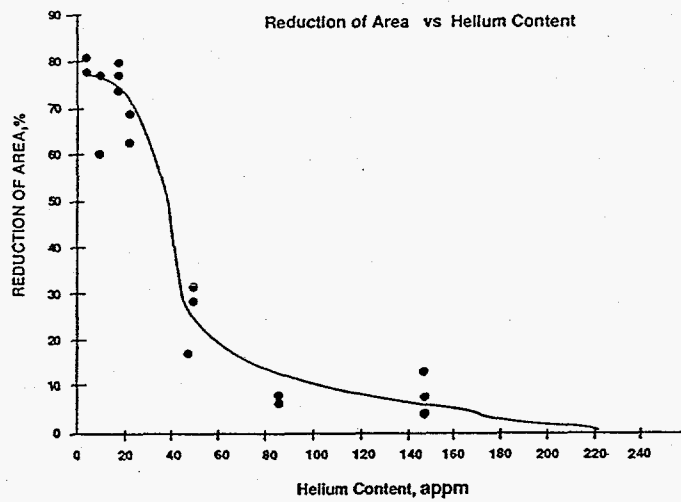


D. Irradiated; Overlay weld;
10 appm helium.

Figure 6. Comparison of weld heat affected zone cracking in tritium tricked and irradiated Type 304 stainless steel samples welded by conventional and weld overlay processes.



A. Type 316LN stainless steel tensile samples tested at 1093 K (Data from Reference 12)



B. Type 304 stainless steel tested after welding by a low penetration overlay welding process (Reference 3)

Figure 7. Effect of helium content on the reduction in area at fracture of austenitic stainless steels.

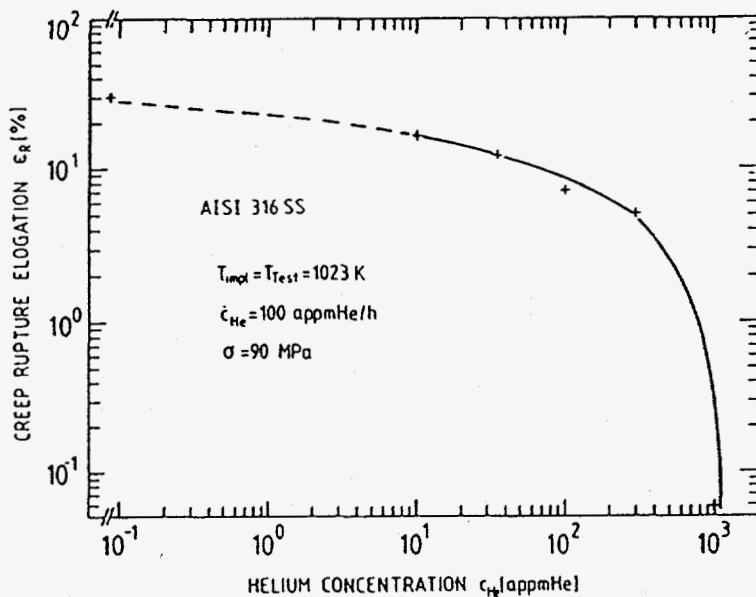
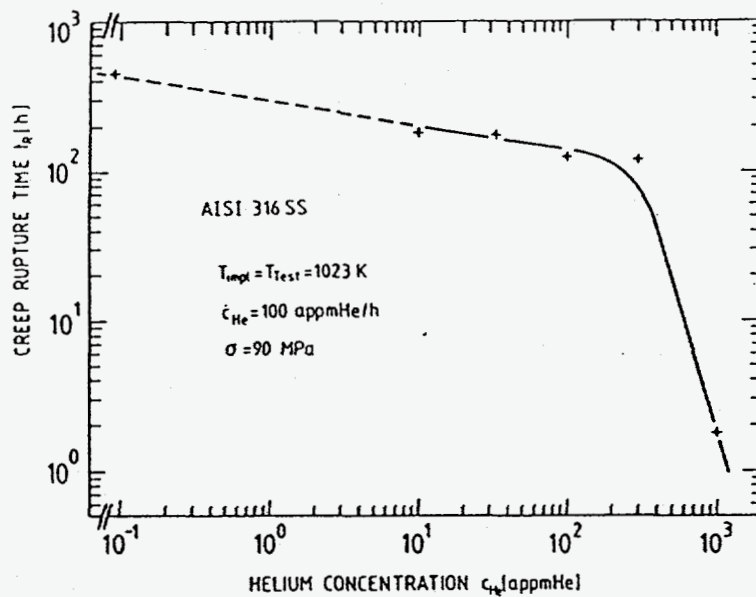


Figure 8. Effect of helium content on the creep rupture behavior of Type 316 stainless steel tested at 1023 K. (After Reference 13)

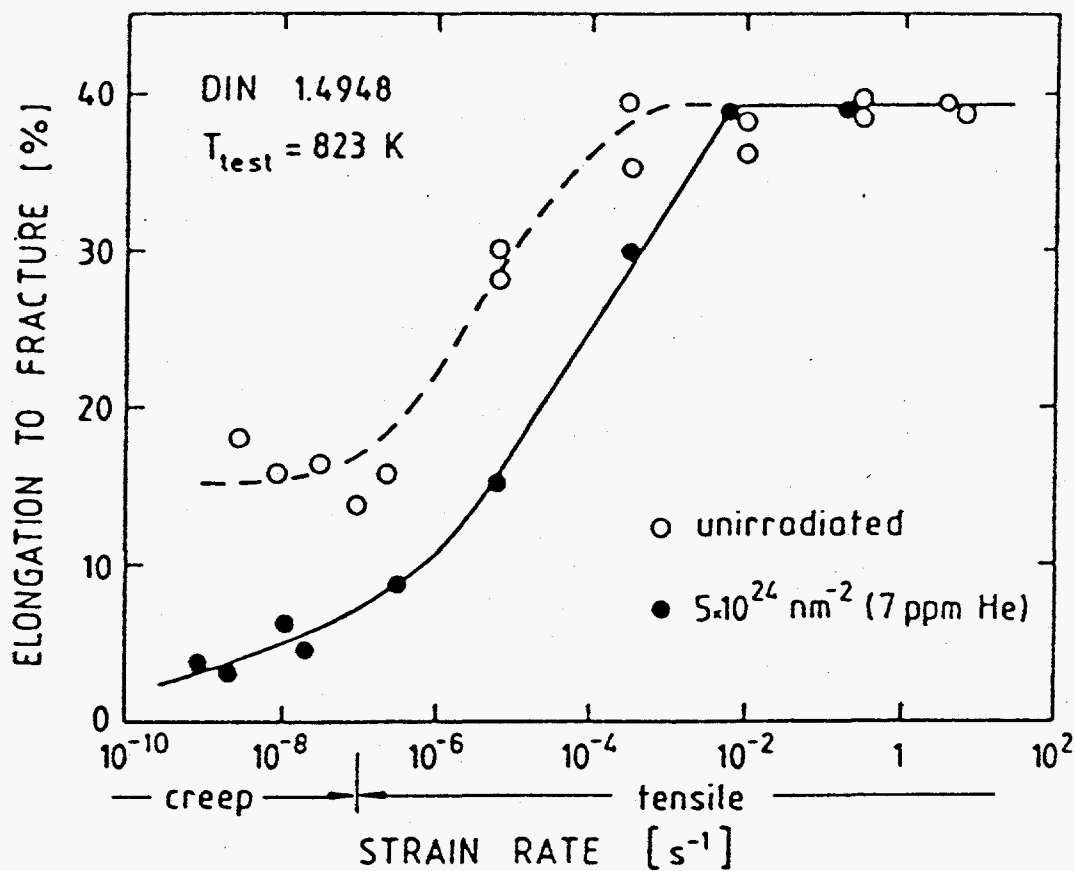


Figure 9. Strain rate dependence of ductility in a stainless steel containing 7 appm He and tested at 823 K (After Reference 13)

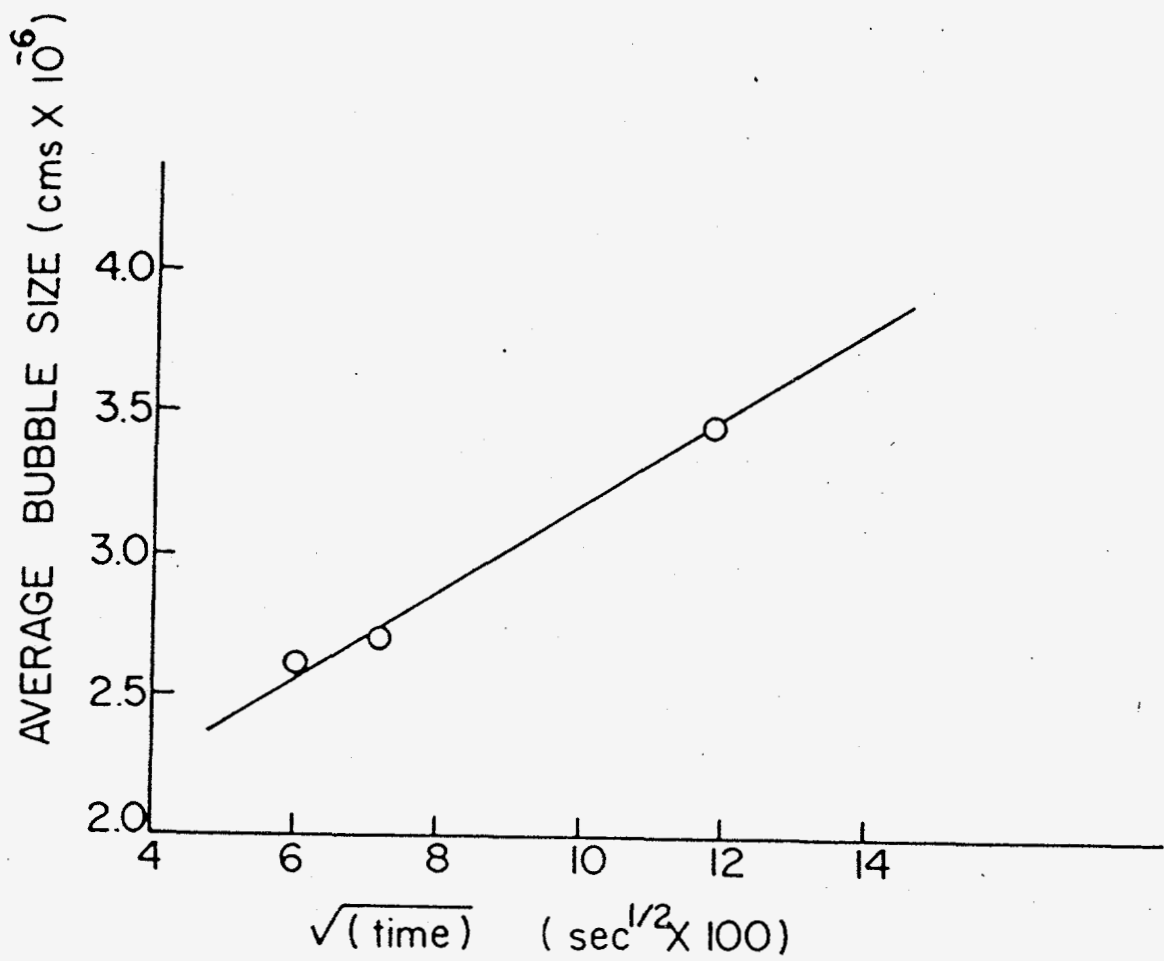


Figure 10. Time dependence of bubble growth in irradiated copper-boron alloy annealed at 1273 K (After Reference 25)

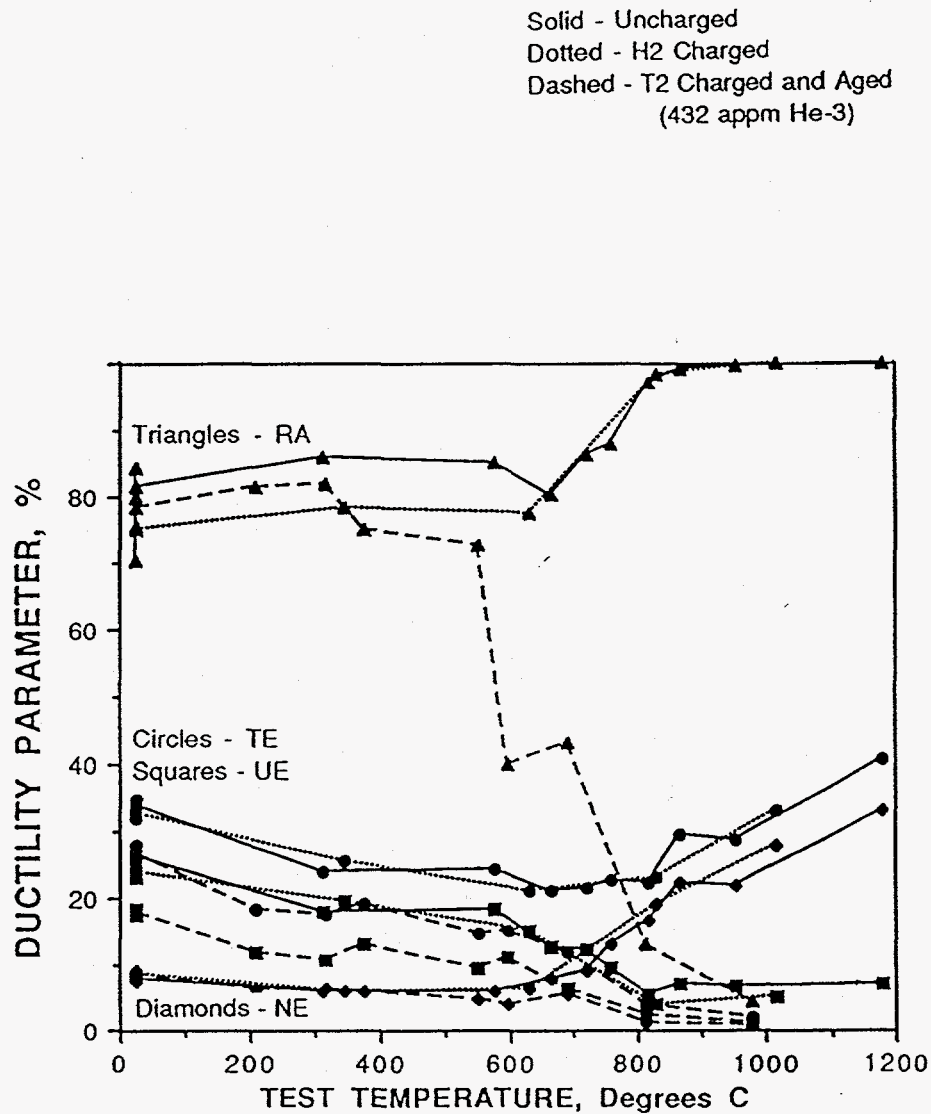
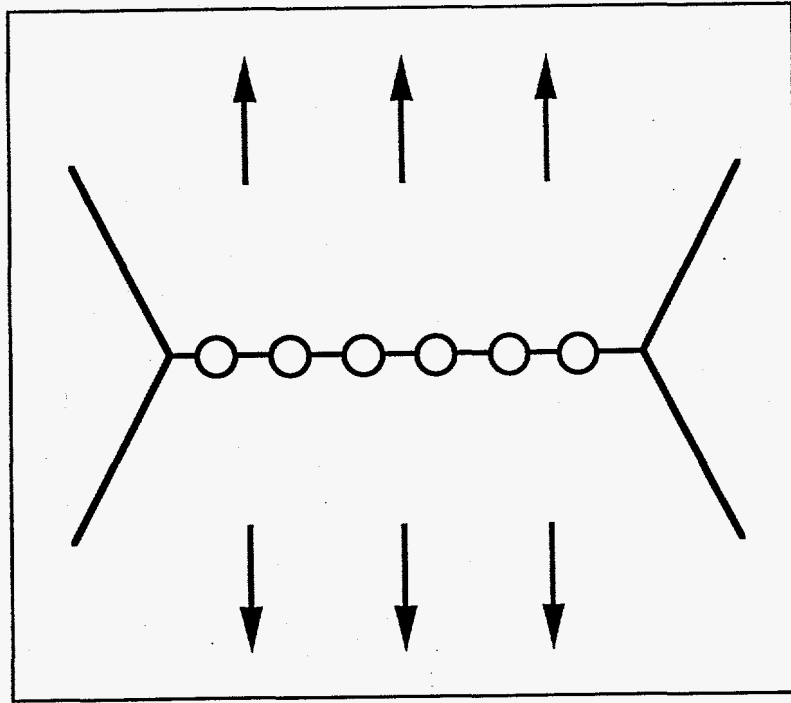
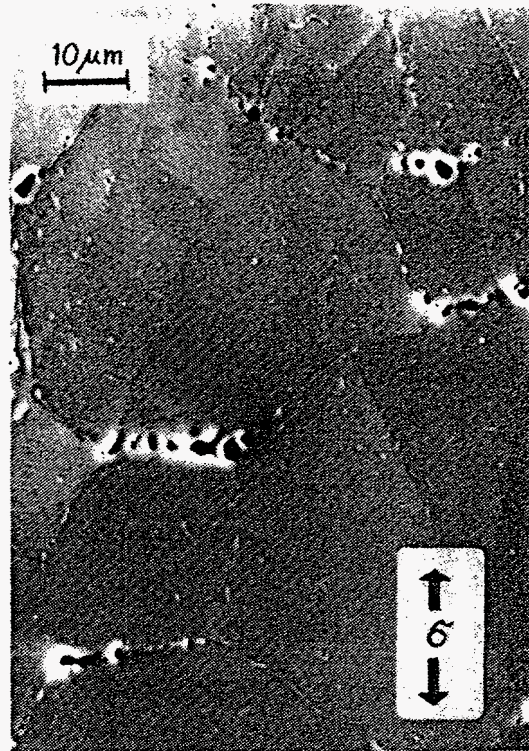


Figure 11. Temperature dependence of tensile ductility in a Type 316 stainless steel containing 432 appm He. (After Reference 12)



A. Schematic of preferential orientation of helium bubbles.



B. Large helium bubbles preferentially located on grain boundaries perpendicular to applied stress (see arrows). (After Reference 13)

Figure 12. Helium bubble development preferentially on grain boundaries oriented perpendicular to an applied tensile stress.

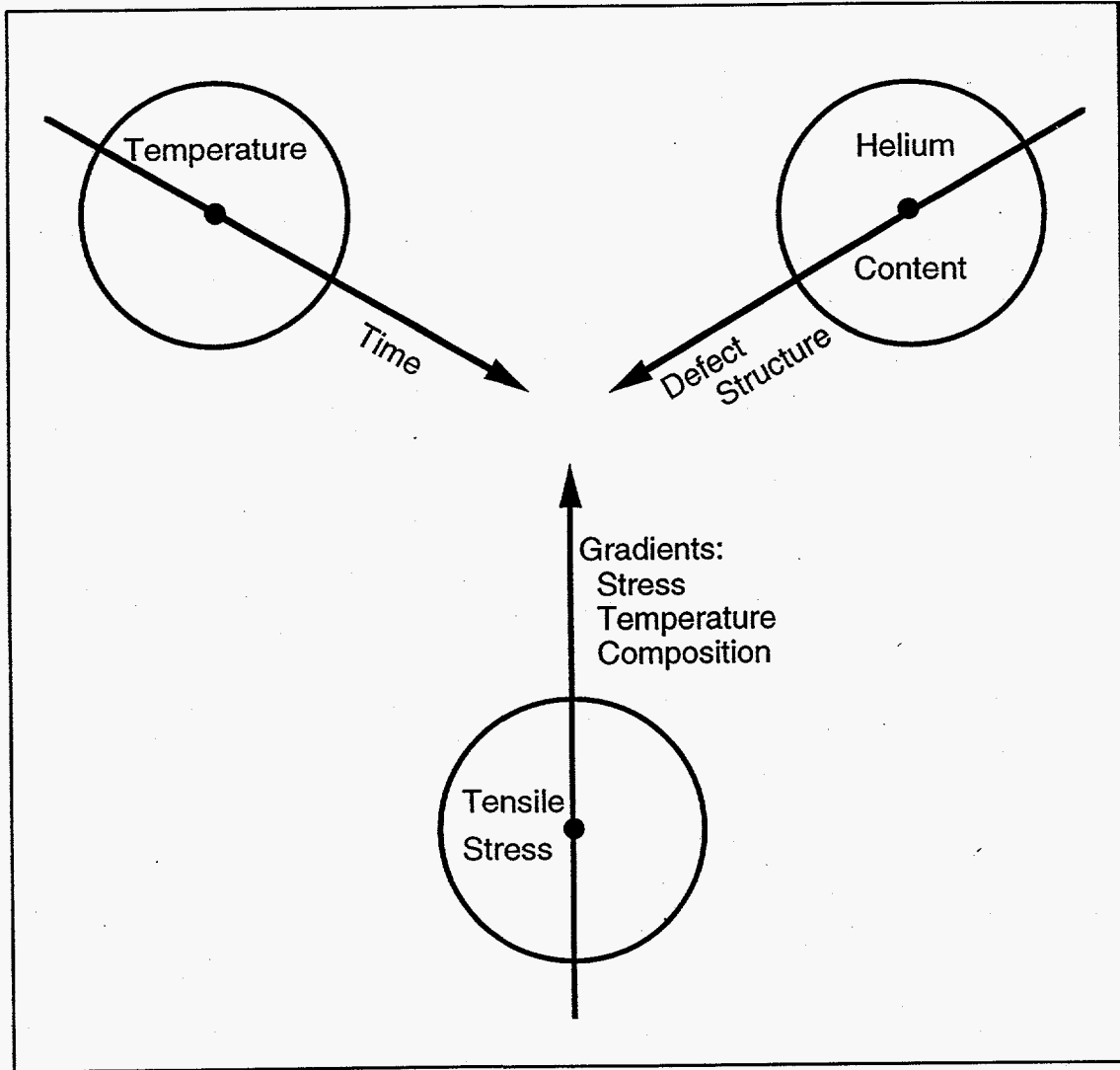


Figure 13. Illustration of variables effecting degradation processes in helium containing materials. Radius of circles increase with increasing temperature, helium content and stress. Position of center of circle moves in direction of arrow with increasing time, defect density, and gradient.

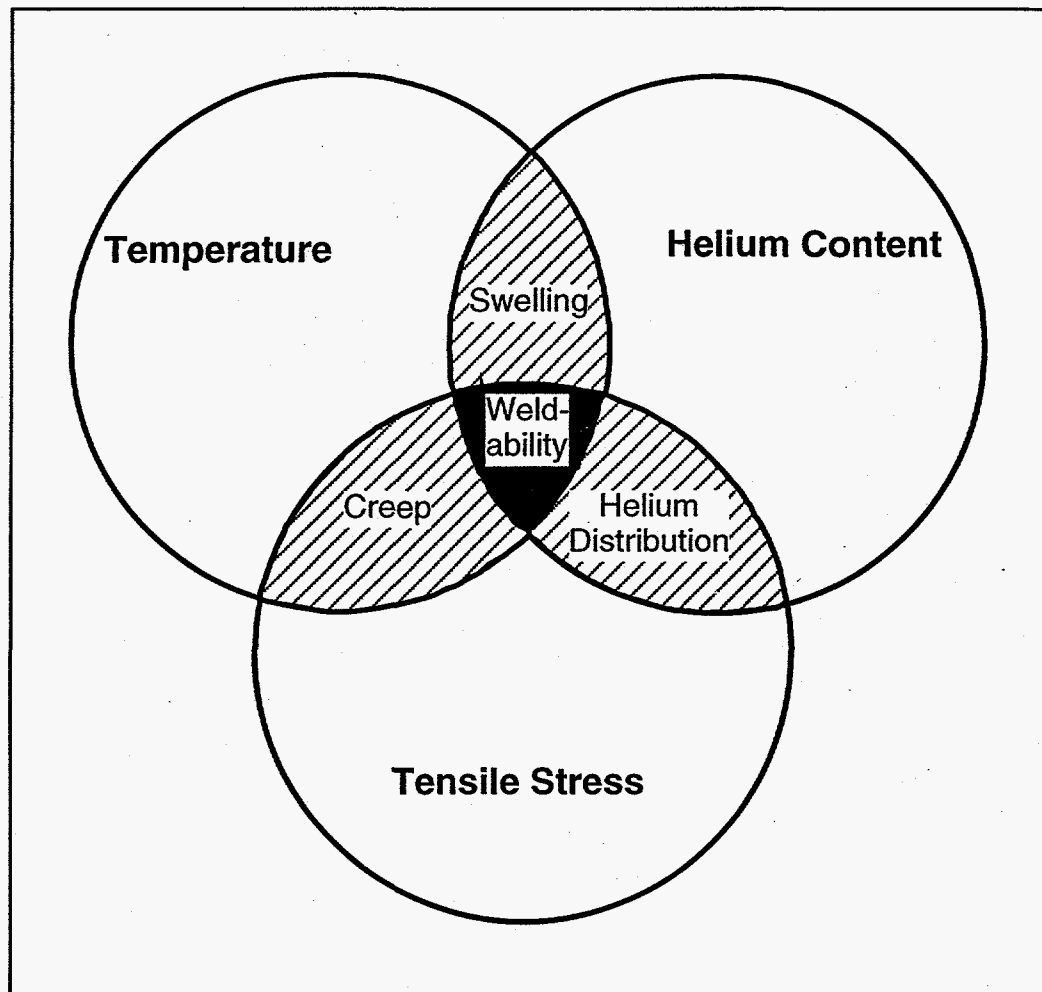


Figure 14. Illustration of the variables influencing swelling, creep and weldability of helium containing materials.

WSRC-TR-97-0031

DISTRIBUTION:

G. Nardella, DOE-OFE
C. C. Baker, U. S. ITER Project Office (UCSD)
K. L. Wilson, SNL-CA
B. Nelson, ORNL
A. F. Rowcliffe, ORNL
M. L. Grossbeck, ORNL

T. M. Tran, 703-A

C. E. Ahlfeld, La Jolla, CA
J. E. Koonce, Japan
F. M. Heckendorn, Japan

R. E. Meadors, 773-41A
B. J. Cross, 773-41A

J. D. Cohen, 773-A
S. L. Tibrea, 773-A

C. R. Wolfe, 773-A
J. R. Knight, 773-A
T. Motyka, 773-A
T. L. Capeletti, 773-41A
C. E. Sessions, 730-A
N. C. Iyer, 773-A
R. L. Bickford, 730-A
D. Z. Nelson, 773-A
S. L. West, 773-A
M. J. Morgan, 773-A

MTS File, 773-A, D-1155
SRTC Records (4), 703-43A